Cent. Eur. J. Eng. • 2(4) • 2012 • 638-650
DOI: 10.2478/s13531-012-0029-x

VERSITA

Central European Journal of **Engineering**

# Experimental and analytical study of high velocity impact on Kevlar/Epoxy composite plates

**Research Article**

Rahul S. Sikarwar[1], Raman Velmurugan[1]*, Velmuri Madhu[2]

*1 Dept. Of Aerospace Engineering, IIT Madras, Chennai, Tamilnadu, 600036*

*2 Defense Metallurgical Research Laboratory, Hyderabad, Andhra Pradesh*

**Received 16 April 2012; accepted 26 June 2012**

**Abstract:** In the present study, impact behavior of Kevlar/Epoxy composite plates has been carried out experimentally by considering different thicknesses and lay-up sequences and compared with analytical results. The effect of thickness, lay-up sequence on energy absorbing capacity has been studied for high velocity impact. Four lay-up sequences and four thickness values have been considered. Initial velocities and residual velocities are measured experimentally to calculate the energy absorbing capacity of laminates. Residual velocity of projectile and energy absorbed by laminates are calculated analytically. The results obtained from analytical study are found to be in good agreement with experimental results. It is observed from the study that 0/90 lay-up sequence is most effective for impact resistance. Delamination area is maximum on the back side of the plate for all thickness values and lay-up sequences. The delamination area on the back is maximum for 0/90/45/-45 laminates compared to other lay-up sequences.

**Keywords:** Kevlar • Epoxy composite plates • Velocity



## 1. Introduction

Fiber reinforced polymer composites are widely used in personal armors, helmets and combat vehicles. One of the major applications of Kevlar fibers is in personnel armor due to its light weight, high stiffness and high energy absorbing capacity. Personnel armors usually are subjected to high velocity bullet impact so while designing the personnel armors energy absorbing capacity of plates is important to know. Energy absorbing capacity of composites depends on many factors like fiber properties, matrix properties, interfacial strength, thickness, fiber orientations etc. Energy of bullet is absorbed by different damage mechanisms like fiber failures [1, 9, 13], elastic deformation of fibers [9, 13], delamination and matrix cracking [1, 3, 13], and cone formation [9, 13]. By knowing the energy absorption by different damage mechanisms residual velocity of projectile can be calculated. Zhu *et al.* [1] have done the quasi-static and dynamic experimental investigation of Kevlar/Polyester laminates of different lay-ups and thickness values which were subjected to different speed of sharp cylindro-conical projectiles and concluded that fiber failure and local deformation are major energy absorbing mechanisms. They also observed that global and shear stiffness play major role in resisting quasi static penetration while it is least effective in dynamic penetration. Ganesh Babu *et al.* [2] have done impact test using heavy mass projectile using

*E-mail: ramanv@iitm.ac.in



Springer

round, conical and flat nose shape projectiles on unidirectional Glass/Epoxy composite plates. They concluded that on thin laminates nose shape has little influence on ballistic limit and energy absorbing capacity while thick nose has higher effects. Mines *et al.* [3] have investigated experimentally the effect of projectile geometries, thickness of laminates and mass of projectile on Glass/Polyster laminates and showed that impact perforation energy is highest for flat cylindrical projectile when compared to cone and hemispherical projectiles. They have also shown that energy absorbed by delamination, plays important role when thickness of laminates increases. Hazel *et al.* [4] have compared the energy absorbing capacity of two bonded CFRP laminates and single laminates of same thicknesses impacted by high velocity steel sphere and concluded that bonded laminates are showing improved impact performance. Lopez-Puente *et al.* [5] have presented the normal and oblique penetration of CFRP laminates using both experimental and the finite element commercial code Abaqus/Explicit. They used damage criteria based on Chang-Chang modified theory [6] for woven laminates and validated with experimental results. It is concluded that below the ballistic limit, the damage extent for normal impact is larger than that for the oblique impact. The damage extent at higher velocities appeared to be greater for oblique impacts. Well above the ballistic limit, the residual velocity is not a[U+FB00]ected by the impact obliquity since the main energy absorbing mechanism is the linear momentum transfer. Above the ballistic limit the damage extent decreases with impact velocity. Gower *et al.* [7] have done experimental and numerical investigation of backplane displacement of Kevlar/Epoxy composite laminates impacted by hemispherical and conical projectiles. Sevkat *et al.* [8] have carried out combined experimental and numerical study of impact damage of cross ply and angle ply laminated composite panels, made of glass fiber and toughened epoxy. They used LS DYNA with modified user defined non linear orthotropic damage model and Chang-Chang linear orthotropic model to simulate experimental results. Morye *et al.* [9] developed a simple analytical model to determine the energy absorbed by composites in ballistic impact and ballistic limit. The values of ballistic limit have been compared with experimentally determined values for Nylone 66 fibers and Dyneema UD66. Smith *et al.* [10] have developed analytical model for transverse wave propagation in the yarns of infinite length where there are no clamps to reflect the waves. They observed that the impact initiates a variable strain that propagates down the filament between an ‘elastic wave’ front and ‘plastic wave’ front. A transverse wave, shaped like an inverted ‘V’, then travels in the constant strain region behind the plastic wave front. Parga-landa *et al.* [? ] developed an analytical model for soft armors that can be used to calculate tension, displacement and velocity in each layer and projectile, yarn stresses and strains and the damage area by finite difference approach. Bohong Gu [12] has also developed analytical model to calculate the decrease in kinetic energy and residual velocity of projectile penetrating targets composed of multilayered planer woven fabric of Twaron and Kuralon. Compared with other models, the perforation time in this model has been estimated from the time, during which failure strain at a given strain rate is generated. But the effect of projectile shape has not been taken into account. Naik *et al.* [13] have analyzed experimentally and analytically the ballistic behavior of Glass/Epoxy composite laminates impacted by flat ended cylindrical. Zhu *et al.* [14] have also presented an analytical model for normal impact and perforation of conically tipped hard steel cylinder on laminated Kevlar-29/Polyester targets. They used laminated plate theory to calculate global deflection of the plate. The finite difference technique has been used to determine local deformation, fiber and matrix failure as well as motion of projectile. Chocron-Benloulo *et al.* [14] have developed one dimensional simple analytical model for ballistic impact against ceramic/composite armors and verified the results with experimental and numerical simulations.

The objective of the present paper is to investigate experimentally and analytically the effect of fiber orientation and thickness on energy absorbing capacity of Kevlar/Epoxy composite laminates. An analytical study has been carried out based on energy conservation law. Using this formulation total energy absorbed, ballistic limit of laminates and residual velocity of projectile are determined. For experimental investigation, laminates of different thicknesses and orientations have been prepared and tested for residual velocity with initial velocity of projectile of about 400 m/sec. Results obtained from both analytical and experimental investigations have been compared.

## 2. Material and specimen fabrication

Kevlar is the most commonly used fiber for ballistic resistance applications and woven is most widely used architecture for the given purpose. So in the present work composite laminates are prepared by 165 gsm Kevlar-29 woven fabrics and Epoxy resin (Araldite LY- 556 and hardener HY-951). Laminates were prepared using hand lay-up and compressed using compression moulding machine. Laminates prepared were of 8, 12, 15 and 19 plies for achieving different thickness values. Each laminate of a particular thickness was prepared for four different orientations that include 0/90, 0/90/30/-60, 0/90/45/-45 and 30/-60/60/-30. The specimen sizes of 300 mm × 300 mm were prepared

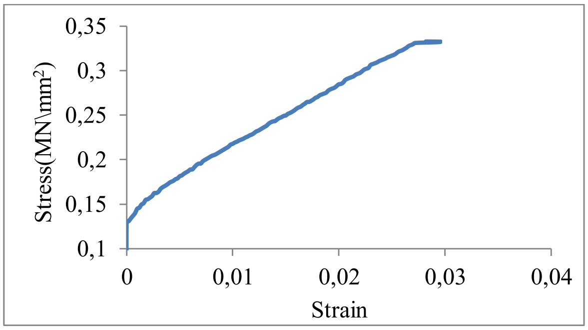


**Figure 1.** Stress-Strain diagram of Kevlar/Epoxy specimen(0/90).

**Figure 2.** 9 × 19 mm Parabellum bullets.

**Table 1.** Material properties 0/90 lay-up for Kevlar/Epoxy composite.

| $E_1$ (GPa) | $X_{1t}$ (Mpa) | $E_2$(GPa) | $\varepsilon_f$ (%) | $\nu_{12}$ | $G_{II}$ (J/m$^3$) |
|---|---|---|---|---|---|
| 33.5 (7%) | 350 (7%) | 8.0 (5%) | 3 | 0.3 (10%) | 500 |

for this study. Each layer of the plate has an average thickness of 0.3 mm. To determine the material properties, such as tensile modulus (Figure 1), shear modulus, Poisson's ratio and fracture toughness in Mode-II, basic tests have been conducted according to ASTM standards. For each property, five specimens were tested. Properties obtained from the tests of 0/90 laminates has been summarized in Table 1.

## 3. Experiments

The experiments were conducted on laminates made from 8, 12, 15 and 19 layers. Laminates prepared for each thickness are made from four orientations and are subjected to impact against given projectile. Composite panels were held on target holder at 10 m distance from muzzle end of the gun. The velocity of bullet is 390 ±10 m/sec. Figure 2 Shows 9 × 19 mm Parabellum bullets.

For each set of lay-up and thickness, five sets of readings have been taken for each initial velocity and residual velocity. Impact velocities and corresponding residual velocities for different lay-ups and thicknesses have been summarized and are given in Tables 2 to 5.

From Table 2, it is observed that average energy absorption has increased with increase in thickness value; the energy absorbed by each layer is also increasing with increasing thickness of the laminates.

From Table 3, it can be understood that the 0/90/30/-60 layered laminates also show similar kind of energy absorbing trends as that of cross ply laminates but less than cross ply laminates.

Table 4, which corresponds to 0/90/45/-45 layer laminates shows similar trends as the previous laminates. The energy absorption is slightly less than the previous laminates.

The 30/-60/60/-30 laminates also show similar trends as other laminates and energy absorption is less than the other laminates. Results are given in Table 5.

From the Tables 2 to 5 it is clear that energy absorbing capacity and energy absorbed by each layer of laminates increased for all lay-ups with increase in thickness values. It is also observed that for same thickness, energy absorbing capacity is decreasing as the orientations of layers are varied from 0/90, 0/90/30/-60, 0/90/45/-45 to 30/-60/60/-30. This is because plate's effective modulus in two perpendicular direction decreases when the orientation is changed from 0/90 to 30/-60/60/-30.

It's observed that for all lay-ups and thicknesses, damage on the front side of the plate is smaller than the damage on the back side. In the front side the damage shape is like a hole having a diameter nearly equal to bullet diameter. Delamination area is also small and circular in shape, around the hole, as shown in Figures 3 and 4.

Figures 5 to 8 illustrate the damage area on the rear side of the plates for different lay-up sequences for laminate made from 19 layers. It's observed that the directions of cracks on the back side are perpendicular to the direction of fibers. For the same thickness, delamination area is maximum for 0/90/45/-45 lay-up when compared to other lay-up laminates.

Figures 9 to 12 illustrate the damage shape and delamination area on the back side of plates for 0/90 lay-up and different thickness values.

The variation of delamination area on the back side of plates for different lay-ups and thicknesses have been summarized in Figure 13. The values are obtained by using halogen lamps on the back side of the delaminated surface of the plate. It is observed that delamination area on the back side of the plate is maximum for 0/90/45/-45 lay-up sequences and for all thickness values, while 0/90 lay-up is

**Table 2.** Initial and residual velocities for laminates of 0/90 lay-up sequence.

| Layers | Thickness (mm) | Impact velocity (m/s) | Residual average velocity (m/s) | Energy Absorption (J) | Energy absorbed by each layer(J) |
|---|---|---|---|---|---|
| 8 | 2.4 | 378 ± 10 | 374 ± 10 | 11.2 | 1.4 |
| 12 | 3.6 | 381 ± 8 | 374 ± 9 | 21.5 | 1.8 |
| 15 | 4.5 | 378 ± 20 | 367 ± 18 | 29.3 | 1.9 |
| 19 | 5.4 | 376 ± 9 | 360 ± 5 | 43.6 | 2.3 |

**Table 3.** Initial and residual velocities for laminates of 0/90/30/-60 lay-up sequence.

| Layers | Thickness (mm) | Impact velocity (m/s) | Residual average velocity (m/s) | Energy Absorption (J) | Energy absorbed by each layer(J) |
|---|---|---|---|---|---|
| 8 | 2.4 | 386 ± 10 | 382 ± 11 | 11.0 | 1.40 |
| 12 | 3.6 | 377 ± 10 | 372 ± 10 | 18.9 | 1.58 |
| 15 | 4.5 | 385 ± 7 | 376 ± 6 | 24.8 | 1.65 |
| 19 | 5.4 | 382 ± 6 | 370 ± 5 | 35.0 | 1.84 |

**Figure 3.** Damage area at front face of 0/90.

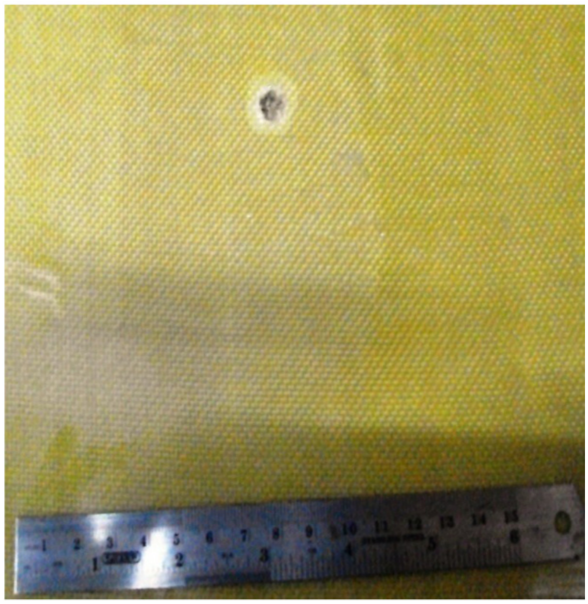

**Figure 4.** Damage area at front face of 30/-60/60/-30.

showing the least delamination area. Delamination area at the rear side of the plate is maximum for 0/90/45/-45 lay-up plates because for these plates interlaminer shear stresses are maximum compared to other orientations and hence matrix failure and delamination are also maximum. For all lay-up sequences of 8 layer laminates the delamination area is almost the same. For same orientation, the damage area on the rear side of the plate increases with increasing number of layers. The reason is that when the projectile impacts on composite laminates initially up to certain thickness of laminate, material surrounding the projectile will undergo compression-shear failure mode [16] and for the remaining thickness of the plate, it will undergo tension-shear failure mode, which is responsible for delamination and matrix cracking on the back side of the composite laminate. If the thickness of laminate is less, then most part of the thickness from the front side of the laminate will fail under compression-shear mode while the remaining small thickness will fail under tension-shear mode which is responsible for delamination hence delamination will be less on the back side of the thin laminate and it increases with increase in thickness of laminate.

**Table 4.** Initial and residual velocities for laminates of 0/90/45/-45 lay-up sequence.

| Layers | Thickness (mm) | Impact velocity (m/s) | Residual average velocity (m/s) | Energy Absorption (J) | Energy absorbed by each layer(J) |
|---|---|---|---|---|---|
| 8 | 2.4 | 386 ± 2 | 383 ± 3 | 9.16 | 1.1 |
| 12 | 3.6 | 382 ± 13 | 376 ± 12 | 16.17 | 1.3 |
| 15 | 4.5 | 375 ± 6 | 366 ± 9 | 24.12 | 1.6 |
| 19 | 5.4 | 383 ± 8 | 371 ± 10 | 33.24 | 1.74 |

**Table 5.** Initial and residual velocities for laminates of 30/-60/60/-30 lay-up sequence.

| Layers | Thickness (mm) | Impact velocity (m/s) | Residual average velocity (m/s) | Energy Absorption (J) | Energy absorbed by each layer(J) |
|---|---|---|---|---|---|
| 8 | 2.4 | 381 ± 10 | 378 ± 9 | 9.0 | 1.12 |
| 12 | 3.6 | 386 ± 11 | 381 ± 11 | 14.3 | 1.2 |
| 15 | 4.5 | 388 ± 8 | 381 ± 9 | 20.6 | 1.3 |
| 19 | 5.4 | 390 ± 6 | 380 ± 10 | 27.9 | 1.4 |

**Figure 5.** Damage at rear face of 0/90, 19 layer laminate.

**Figure 6.** Damage on rear face of 0/90/30/-60, 19 layer laminate.

As is seen in Figure 14, the maximum energy is absorbed by the 0/90 lay-up laminate and it is minimum for the laminate of 30/-60/60/-30 lay-ups for all thickness values of the laminates while from other orientations, 0/90/30/-60 is more effective in energy absorption when compared to 0/90/45/-45lay-ups. It is also observed that energy absorbing capacity increases with increasing thickness of plates.

## 4. Analytical Model

Analytical model has been developed to predict the residual velocity and ballistic limit of laminates, which is based on simple energy conservation law. By knowing the different failure modes, occurring during perforation of plate, analytical formulation has been carried out to calculate the energy absorbed in each damage mechanism and total energy absorbed by plate. Using the concept of total energy absorbed by damaged plate is equal to reduction in kinetic energy of bullet, residual velocity of the projectile has been determined. When the total energy absorbed by damaged plate is equal to the initial kinetic energy of projectile, ballistic limit of plate is obtained.
For the development of the model following assumptions have been made:

1. Energy absorbed in projectile deformation is negligible compared to total energy absorbed.

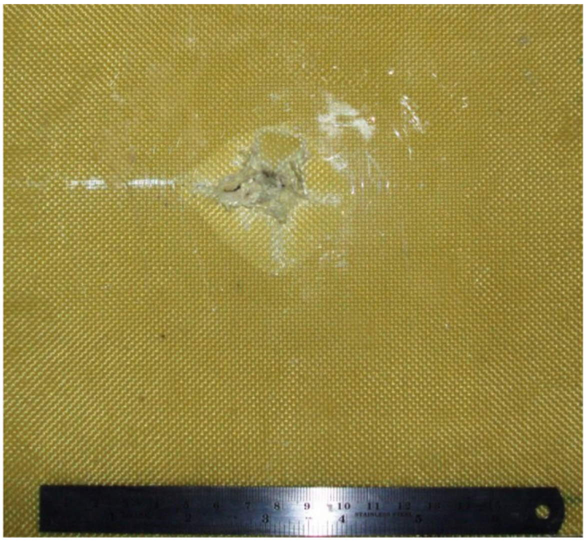

**Figure 7.** Damage at rear face of 0/90/45/-45 19 layer laminate.

**Figure 8.** Damage on rear face of 30/60/30/60 19 layer laminate.

2. Energy lost due to friction between projectile and composite is negligible.
3. Failure mechanism of composite is uniform across the thickness.
4. Fibers in each layer act independently. Fiber failure in one lamina doesn't affect failure in other lamina.
5. Material properties remain constant during impact.
6. Strain rate will remain constant during perforation.

**Figure 9.** Damage on rear side of 19 layers 0/90 plate.

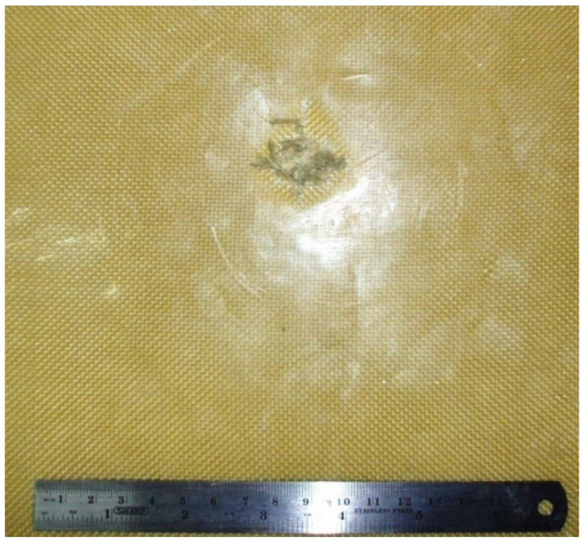

**Figure 10.** Damage on rear side of 15 layers 0/90 plate.

Total kinetic energy of projectile is:

$$KE_{po} = m_p V_0^2 \tag{1}$$

Where $m_p$ is the mass of projectile and $V_0$ is initial velocity of projectile. Some of the projectile energy is absorbed by the laminates by deforming into various failure modes and reduce the velocity of projectile to $V_p$. Thus from energy balance law:

$$\frac{1}{2} m_p V_0^2 = E_0 + \frac{1}{2} m_p V_r^2 \tag{2}$$

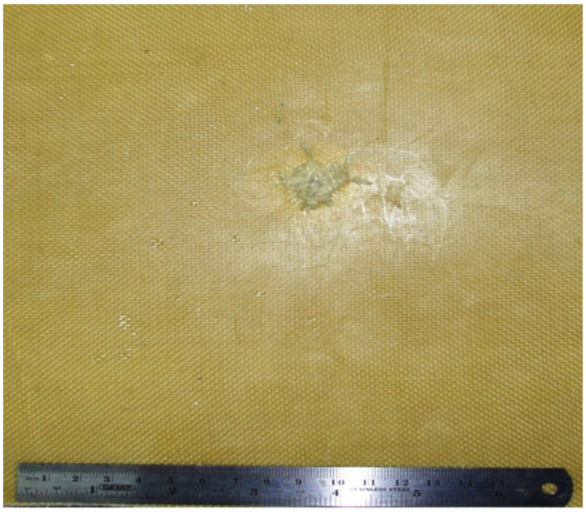

**Figure 11.** Damage on rear side of 12 layers 0/90 plate.

**Figure 12.** Damage on rear side of 8 layers 0/90 plate.

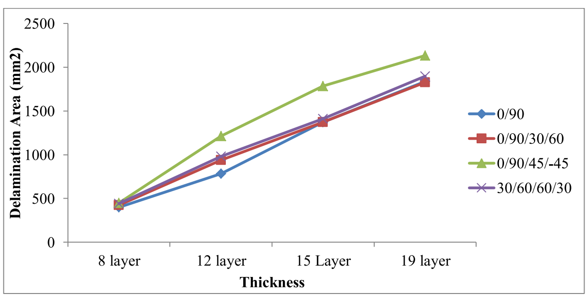


**Figure 13.** Delamination area on back face of plates for different lay-up and thicknesses.

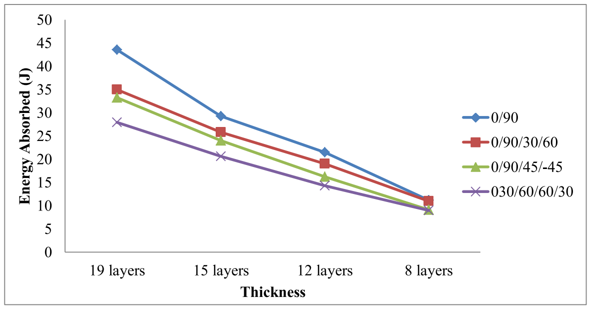


**Figure 14.** Experimentall determined variation of average energy absorbed by plates having a different thicknesses and lay-ups.

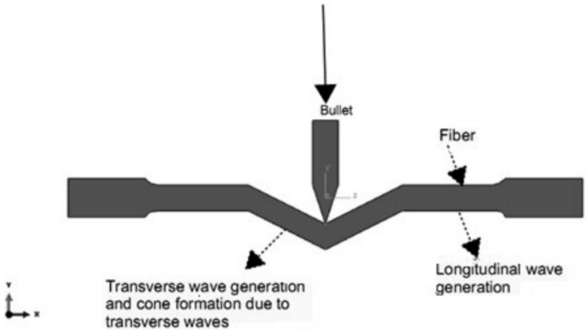


**Figure 15.** Propagation of longitudinal and transverse waves during impact event.

where $E_0$ is the total energy absorbed by different deformation mechanisms of the laminate.

For single yarn of infinite length [10] subjected to impact, an elastic and plastic wave propagates outwardly from the impact point (Figure 15). The velocity of elastic wave propagation is:

$$C_e = \sqrt{\frac{1}{\rho}\left(\frac{d\sigma}{d\varepsilon}\right)}_{\varepsilon=0} \quad (3)$$

And plastic wave front propagation [10] travels slowly with a velocity of

$$C_p = \sqrt{\frac{1}{\rho}\left(\frac{d\sigma}{d\varepsilon}\right)}_{\varepsilon=\varepsilon_p} \quad (4)$$

The propagation of elastic wave is in the radial direction and plastic wave is in the fiber direction from the conical deformed shape on the rear side of the plate. The time taken for the cone formation depends on the strain rate and is given by the expression:

$$\Delta t = \frac{\Delta\varepsilon}{\dot{\varepsilon}} \quad (5)$$

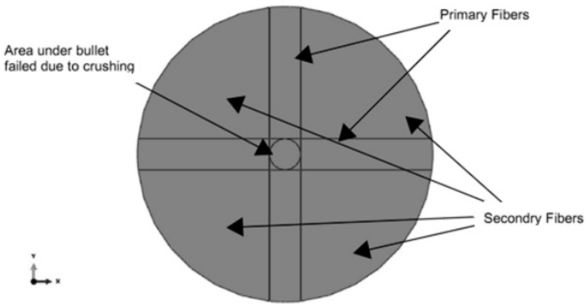


**Figure 16.** Primary and secondary fibers in cone formed on back face of plate.

where

$$\dot{\varepsilon} = \frac{V_0}{L_{gauge}} \tag{6}$$

From this $\Delta_t$, we can get the radius of cone, which is given by the expression:

$$R_c = C_p \Delta_t \tag{7}$$

The value of $C_p$ is calculated from Equation (4).

## 4.1. Energy absorbed in tensile failure of primary yarns

Yarns, which are the collection of filaments, directly under projectile impacting the laminates, are the primary yarns (Figure 16) and fail in tensile mode. Energy absorption during tensile failure of yarns is given by

$$E_{TF} = \frac{\pi d^2 h}{4} E_c + \left(4R_c hd - \frac{\pi d^2 h}{4}\right) E \left(\frac{\varepsilon_p}{2}\right)^2 \tag{8}$$

This is the summation of energy required for failure of circular area under bullet and energy absorbed by plastic deformation of primary yarns. Here $E_c$ is given by the area under the stress-strain curve in uni-axial tensile testing (Figure 1) which is energy required to fail the composite under tensile load.

## 4.2. Energy absorbed in elastic deformation by secondary yarns

All yarns except primary yarns in the deformed cone are considered as secondary yarns which is shown in Figure 16. Secondary yarns deform elastically and absorb some kinetic energy of projectile. Assuming a linear variation of strain within the secondary yarns from the center of the laminate and up to the boundary of the delaminated zone ($R = R_c$), the expression for strain in the secondary yarns is given by:

$$\varepsilon = \frac{\varepsilon_0 (R_c - r)}{R_c} \tag{9}$$

The corresponding energy absorbed in the secondary yarns is given by:

$$E_{ED} = \left(\pi E \varepsilon_0^2\right) \int_0^{R_c} rhdr \tag{10}$$

## 4.3. Energy absorbed due to shear plug formation

When thin plates are subjected to high velocity projectile because of cutting action of projectile, material will fail in shear mode and shear plug will be formed [17], which absorbs some amount of energy. The energy expression for shear plug is:

$$E_{SP} = \pi dh^2 S_{sp} \tag{11}$$

## 4.4. Energy absorbed due to delamination and matrix cracking

During impact on a composite plate, because of different fiber orientations and bending of plate, varying degree of interlaminar shear stresses are generated and that lead to delamination. Compressive waves are generated along the thickness direction which causes matrix cracking. Delamination and matrix cracking absorb some part of kinetic energy of the projectile. Energy absorbed by delamination can be given by:

$$E_{DL} = \pi R_c^2 G_{IIcd} \tag{12}$$

Energy absorbed by matrix cracking is given by:

$$E_{MC} = \pi R_c^2 E_{mt} h V_m \tag{13}$$

where $V_m$ is matrix volume fraction of composites.

## 4.5. Energy absorbed by moving cone

During impact event, transverse waves are generated in fibers and cone is formed on the back side of plate, which will absorb significant amount of kinetic energy of projectile. Energy absorbed by a moving cone on the back face of plate can be expressed in the form:

$$E_{KE} = \frac{1}{16} M_c (V_0 + V_r)^2 \tag{14}$$

The total energy absorbed by the plate by different modes of deformation is given by the expression:

$$E_0' = E_{TF} + E_{ED} + E_{DL} + E_{MC} + E_{KE} + E_{SP} \tag{15}$$

By considering the values of different energies from the Equation (4) to (14) in Equation (15) and using Equation (2), the expression for residual velocity is obtained, which is given by:

$$V_r = \frac{-2M_c V_0 + \sqrt{4M_c^2 V_0^2 - 4(M_c + 8m_p)\left[(M_c - 8m_p)V_0^2 + 16E_0'\right]}}{2(M_c + 8m_p)} \quad (16)$$

where $V_r$ the residual velocity of the projectile after impact. For ballistic Limit, ($V_{50}$), residual velocity should be zero. So Equation (16) can be reduced to

$$V_{50} = \sqrt{\frac{16E_0'}{(8m_p - M_c)}} \quad (17)$$

To predict the residual velocity and ballistic limit for angle ply laminates using the above expressions, it is essential to get the material properties of ply laminates with varying fiber orientations. Using the results obtained by uniaxial tensile tests for 0/90 laminates material properties for angle ply can be calculated.

The modulus values of the laminates for different orientation is obtained by using the expression:

$$Ex = \frac{1}{t}\frac{A_{11}A_{22} - A_{12}^2}{A_{22}} \quad (18)$$

If the laminate is cross ply then:

$$E_x = E_y = \frac{1}{t}\frac{A_{11}^2 - A_{12}^2}{A_{11}} \quad (19)$$

where

$$A_{ij} = \sum_{k=1}^{N} Q_{ij}(h_k - h_{k-1}) \quad (20)$$

$Q_{ij}$ are components of reduced stiffness matrix and $h_k$ is thickness of $k^{th}$ layer.

Table 6 summarizes the energy absorbed by plates of different lay-ups. It can be seen that if the thickness of laminate increases the energy absorbing capacity of the plate also increases. It is observed from Table 6 that for the same thickness maximum energy is absorbed by plates having 0/90 lay-ups while minimum energy is absorbed by 30/-60/60/-30 lay-up plates.

## 5. Comparison of experimental and analytical results

To validate the analytical model, residual velocity and energy parameter 'Energy absorbed/ Initial energy of projectile' have been considered. Results obtained from analytical method have been compared with experimental results.

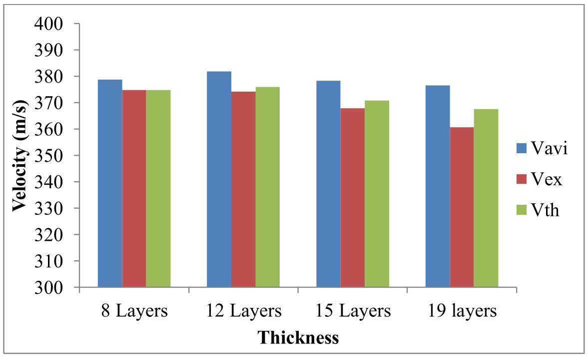


**Figure 17.** Comparison of average residual velocities obtained experimentally and average velocity calculated analytically with initial velocity for (0/90) lay-ups.

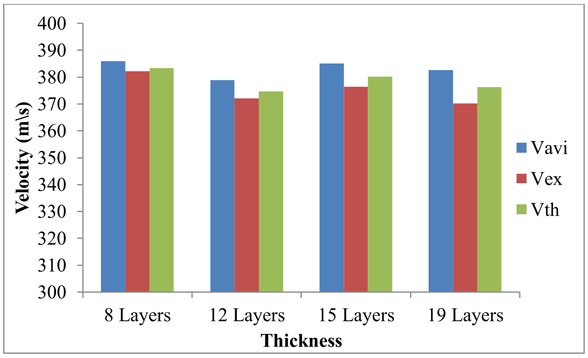


**Figure 18.** Comparison of average residual velocities obtained experimentally and calculated analytically with initial velocity for (0/90/30/-60) lay-ups.

In experiments initial and residual velocities are measured by using infrared sensors. By knowing the residual velocity the energy absorbed by plates can be calculated by using the expression:

$$E = \frac{1}{2}M_P(V_r^2 - V_i^2) \quad (21)$$

From Figure 17, it can be seen that the values of the average residual velocities of experiments match well with that obtained from analytical expressions. The average initial velocity of projectile is varying between 376 m/s to

**Table 6.** Analytically calculated residual velocities for averaged experimental initial velocities.

| Lay-up | Number of layers | Averaged experimental initial velocities (m/s) | Analytically calculated residual velocities(m/s) | Analytically calculated energy absorbed (J) |
|---|---|---|---|---|
| 0/90 | 8 | 378 | 373.2 | 13.52 |
| | 12 | 381 | 373.2 | 22.06 |
| | 15 | 378 | 367.6 | 29.1 |
| | 19 | 376 | 362.7 | 36.8 |
| 0/90/30/-60 | 8 | 386 | 382.5 | 10.1 |
| | 12 | 377 | 370.9 | 17.1 |
| | 15 | 385 | 376.7 | 23.7 |
| | 19 | 383 | 371.3 | 33.1 |
| 0/90 /45/-45 | 8 | 386 | 382.6 | 9.8 |
| | 12 | 382 | 376.1 | 16.8 |
| | 15 | 375 | 367 | 22.3 |
| | 19 | 383 | 371.6 | 32.3 |
| 30/60/30/60 | 8 | 381 | 378.3 | 7.7 |
| | 12 | 386 | 381.4 | 13.2 |
| | 15 | 388 | 381.6 | 18.4 |
| | 19 | 390 | 381.7 | 24.0 |

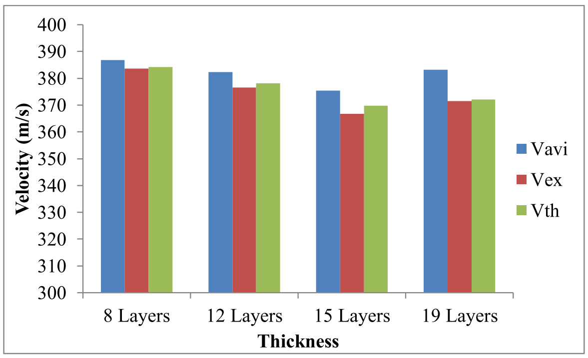


**Figure 19.** Comparison of average residual velocities obtained experimentally and calculated analytically with initial velocity for (0/90/45/-45) lay-up plates.

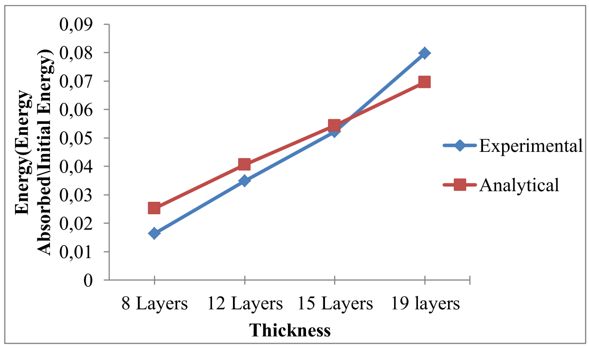


**Figure 21.** Comparison chart for variation in dimensionless parameter with thickness of plates for 0/90 lay-up obtained analytically and experimentally.

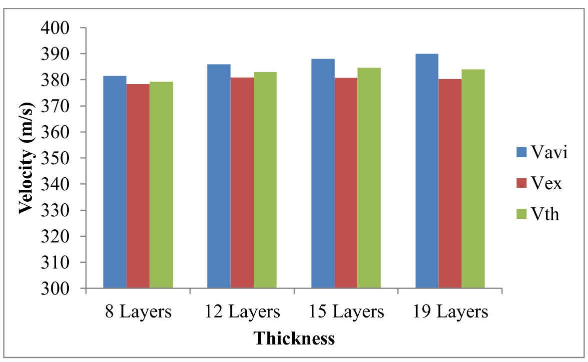


**Figure 20.** Comparison of average residual velocities obtained experimentally and calculated analytically with initial velocity for (30/-60/60/-30) lay-up.

381 m/s. In Figures 17 to 20, $V_{avi}$ is average initial velocity of projectile, $V_{ex}$ is experimentally determined residual velocity and Vth is analytically calculated residual velocity. Figure 18 shows that for all thickness values the residual velocities are showing good correlation between experimental and analytical results. Average initial velocity of projectile is varying between 377 m/s to 386 m/s.

As is seen in Figure 19, it is clear that the averaged experimentally determined residual velocities are showing good agreement with analytically calculated residual values.

Figure 20 corresponds to 30/-60/60/-30 lay-up laminates. It can be seen that the average experimental residual velocities and analytically calculated velocities are showing good agreement. For these laminates average initial velocities are varying between 381 m/s to 390 m/s.

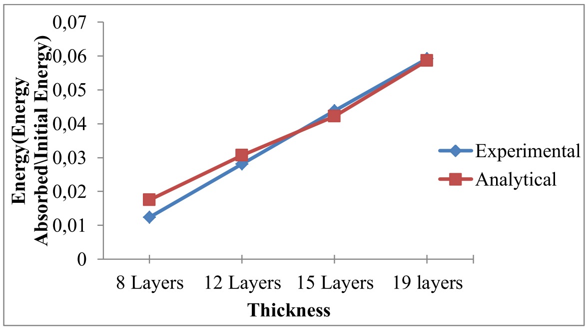


**Figure 22.** Comparison chart for variation in dimensionless parameter with thickness of plates for 0/90/30/-60 lay-up obtained analytically and experimentally.

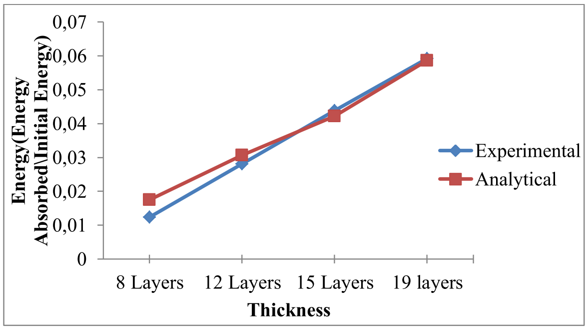


**Figure 23.** Comparison chart for variation in dimensionless parameter with thickness of plates for 0/90/45/-45 lay-up obtained analytically and experimentally.

Figure 21 shows the comparison of dimensionless parameter (Energy absorbed by the plates/ Initial energy of projectile) obtained experimentally and analytically for 0/90 laminates. It shows that experimentally determined values are matching well with analytically calculated values. It is also clear that as the thickness of the plate increases, the energy absorption also increases.

Figure 22 corresponds to the variation of energy, determined experimentally and analytically, for 0/90/30/-60 lay-up laminates of different thickness values when subjected to impact loading. Here also experimental values are showing good correlation with analytical values.

Figure 23 summrizes the variation of energy value for 0/90/45/-45 laminates determined analytically and experimentally.

From Figures 24, which shows the comparison of energy parameter between theoretical and experimental values for 30/-60/60/-30 laminates.

Figures 21 to 24 show the comparison of energy parameter determined experimentally and analytically. It is observed that the analytical model results are matching well with experimental results.

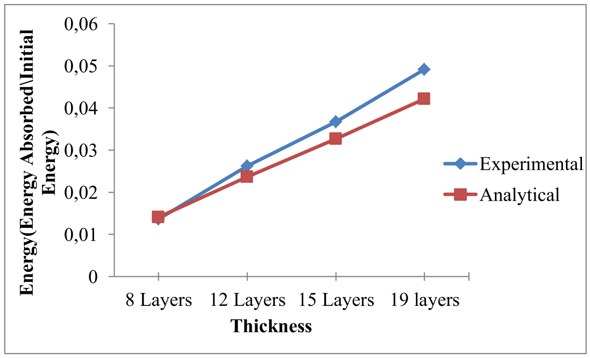


**Figure 24.** Comparison chart for variation of average energy absorbed by different thickness plates of 30/-60/60/-30 lay-up obtained by theoretical and experimental methods.

## 6. Conclusion

In the present work the effect of orientation angle and thickness values on high velocity impact of Kevlar/Epoxy laminates has been studied analytically and experimentally. The following conclusions are drawn from the present study:

1. On the front side of the plate, there is small hole of bullet while on the rear side; damage area is more containing cracks, delamination and matrix cracking.
2. Cracks on the rear side are perpendicular to fiber orientation showing tensile failure of fibers.
3. Delamination area on the rear side is maximum for 0/90/45/-45 laminates when compared to laminates of other lay-up sequences and for different thickness values.
4. Energy absorbing capacity is maximum for 0/90 lay-ups and is minimum for 30/- 60/60/-30 lay-up sequences and for all thicknesses.
5. For all lay-up sequences, energy absorbing capacity and energy absorbed per layer increases with increasing thickness.
6. The damage area on the rear side increases with increasing thickness of the plate.

### Nomenclature

| | |
|---|---|
| $\rho$ | Density |
| $\varepsilon_0$ | Failure strain |
| $\varepsilon_p$ | Plastic strain |
| $\dot{\varepsilon}$ | Strain rate |
| $D$ | Projectile diameter |
| $h$ | Thickness of laminate |
| $R_c$ | Moving cone radius at the end of impact event |
| $M_c$ | Mass of moving cone at the end of impact event |

$E_{TF}$ Energy absorbed in tensile failure mode
$E_{ED}$ Energy absorbed in elastic deformation of secondary yarns
$E_{DL}$ Energy absorbed in delamination
$E_{MC}$ Energy absorbed in matrix cracking
$E_{SP}$ Energy absorbed in shear plug formation
$E_0$ Total energy absorbed in different failure modes
$V_{50}$ Ballistic limit of laminate
$V_r$ Residual velocity of projectile
$m_p$ Mass of projectile
$G_{II}$ Mode II critical strain energy release rate
$E_{MT}$ Matrix cracking energy per unit volume
$V_m$ Matrix volume fraction
$V_{avi}$ Averaged experimental initial projectile velocity
$V_{th}$ Analytically calculated residual velocity
$E_{ex}$ Experimentally determined residual velocity

## Acknowledgments

Experimental work has been carried out at Defense Material Research Lab, Hyderabad. Authors would also like to thank Mr. R. Subba Reddy and technical staff for their sincere support in conducting the experiments.

### References

[1] Zhu G., Goldsmith W., Dharan C.H.K., Penetration of laminated Kevlar by projectiles- I. Experimental investigation, Inter. J. Solids Struct., 1992, 29(4), 399–420

[2] Ganesh Babu M., Velmurugan R., Gupta N.K., Energy absorption and ballistic limit of targets struck by heavy projectile. Latin Am. J. Solids Struct., 2006, 3, 21–39

[3] Mines R.A.W., Roach A.M., Jones N., High velocity perforation behavior of polymer composite laminates, Inter. J. Impact. Eng., 1999, 22, 561–588

[4] Hazell P.J., Appleby-Thomas G.J., Kister G,. Impact, penetration, and perforation of a bonded carbon-fibre-reinforced plastic composite panel by a high-velocity steel sphere: an experimental study. J. Strain Anal. 45. Special issue paper 439

[5] Lopez-Puente J., Zaera R., Navarrao C., Experimental and numerical analysis of normal and oblique ballistic impacts on thin carbon/epoxy woven laminates, Compos. Part A, 2008, 39, 374–387

[6] Chang F.K., Chang K.Y., A progressive damage model for laminated composites containing stress concentrations, J. Comps. Maters., 1987, 21(9), 834–855

[7] Gower H.L., Cronon D.S., Plumtree A., Ballistic impact response of laminated composite panels, Inter. J. Impact. Eng., 2008, 35(9), 1000–1008

[8] Sevkat E., Liaw B., Delale F. , Raju B.B., A combined experimental and numerical approach to study ballistic impact response of S2-glass [U+FB01]ber/toughened epoxy composite beams, Compos. Sci. Technol., 2009, 69, 965–982

[9] Morye S.S., Hine P.J., Duckett R.A., Carr D.J., *et al.*, Modelling of energy absorbtion by polymer composites upon ballistic impact, Compos. Sci. Technol., 2000, 60, 2631–2642

[10] Smith J.C., McCrackin F.L., Schiefer H.F., Stress strain relationships in yarns subjected to rapid impact loading. Part V, Tex. Res. J. 1957, 288–302

[11] Paga-Landa B., Hernandez-Olivares F., An analytical model to predict impact behavior of soft armours, Inter. J. Solids. Struct., 1995, 16(3), 455–466

[12] Bohong G., Analytical modeling for the ballistic perforation of planer plain-woven fabric target by projectile, Compos. Part B, 2003, 34, 361–371

[13] Naik N.K., Shrirao P., Composite structures under ballistic impact, Compos. Struct., 2004, 66, 79–590

[14] Zhu G., Goldsmith W., Dharan C.H.K., Penetration of laminated Kevlar by projectiles-II. Analytical model, Inter. J. Solids Struct., 1992, 29(4), 421–436

[15] Benloulo I.S.C, Sanchez-Galvez V., A new analytical model to simulate impact onto ceramic/composite armours. Inter. J. Solids Struct., 1998, 21(6), 461–471

[16] Gama B.A., Gillespie Jr. J.W., A quasi-static penetration model of ballistic penetration of thick-section composites. 52, 20th annual technical conference, American society for composites, Philadelphia, PA; September 7–9, 2005

[17] Falanagan M.P., Zikry M.A., Wall J.W., El-Shiekh A., An experimental investigation of high velocity impact and penetration failure modes in textile composites. J. Compos. Mater., 1999, 33, 1080–1103